

3D geometry of the strain-field at transform plate boundaries: Implications for seismic rupture

P. Bodin

Center for Earthquake Research and Information, University of Memphis, Memphis, TN

R. Bilham

CIRES and Department of Geological Sciences, University of Colorado, Boulder, CO

Abstract. We examine the amplitude and distribution of slip on vertical frictionless faults in the zone of concentrated shear strain that is characteristic of transform plate boundaries. We study both a 2D and a 3D approximation to this strain field. Mean displacements on ruptures within the zone of concentrated shear strain are proportional to the shear strain at failure when they are short, and are limited by plate displacements since the last major earthquake when they are long. The transition between these two behaviors occurs when the length of the dislocation approaches twice the thickness of the seismogenic crust, approximately the breadth of the zone of concentrated shear strain observed geodetically at transform plate boundaries. This result explains the observed non-linear scaling relation between seismic moment and rupture length. A geometrical consequence of the 3D model, in which the strain-field tapers downward, is that moderate earthquakes with rupture lengths similar to the thickness of the crust tend to slip more at depth than near the surface. Seismic moments estimated from surface slip in moderate earthquakes ($M \leq 7$) will thus be underestimated. Shallow creep, if its along-strike dimension is extensive, can reduce a surface slip deficit that would otherwise develop on faults on which $M < 7$ events are typical. In the absence of surface creep or other forms of off-fault deformation great earthquakes may be necessary features of transform boundaries with downward-tapering strain-fields.

Introduction

Shear strain accumulating within a transform plate boundary is observed geodetically as a velocity field with a profile across the region that approximates an arctangent function (Lisowski *et al.*, 1991). More than 90% of relative plate boundary displacement may be manifest within the resulting narrow region of high shear strain rate, a "strain-channel". The velocity field gradient in California, for example, varies in breadth from less than 50 km to more than 120 km (Lisowski *et al.*, 1991; Robaudo and Harrison, 1993). Where the velocity field is broad, slip at the plate boundary typically occurs on several parallel active fault systems. The surface velocities across the plate boundary may be readily explained as the elastic deformation field manifest on the surface of a half-space caused by antisymmetric displacement on a buried strike-slip fault (Lisowski *et al.*, 1991). Although this geometric model is frequently invoked to explain geodetic observations, the nature of the driving geometry is resolved poorly by geodetic observations. Moreover, uniform slip on a horizontal detachment, or slip on a vertical fault below a

locking depth, generate identical surface velocity fields (Savage, 1990).

We consider two end-member elastic models to investigate a range of possible conditions driving slip on faults inside the strain field associated with the plate boundary velocity field. We refer to the first model as a 2D strain-channel model. We consider the two plates to be rigid rectangular blocks of infinite length separated by a rectangular elastic channel within which strain is developed and released (Figure 1a). Within the 2D strain-channel, contours of equal velocity, displacement and strain are vertical and parallel to the plate boundary. In a 3D strain-channel model, we consider strains associated with the plate boundary to be generated by uniformly-distributed steady slip on a vertical fault below some locking depth in a uniform elastic half-space (Figure 1b). Due to the proximity of the dislocation below the locking depth, contours of equal velocity and displacement in this model converge toward the base of the elastic crust (Figure 1b). Details of the convergence depend somewhat on the distribution of slip on the deeper fault. In the models that follow we consider the simplest case: an isolated rupture growing within a uniform strain field, and defer more complicated and specific models of fault interaction within time-varying strain fields for later work. We estimate the slip distribution and hence the mean slip on frictionless dislocations of different lengths within these systems using boundary-element methods (Crouch and Starfield, 1983; Gomberg and Ellis, 1994).

2D Strain-Channel

Two rigid blocks impose edge shear tractions to a rectangular region of uniform elastic material with breadth B , and thickness W , corresponding to the width of frictionless vertical faults (Figure 2). The boundary element method is used to calculate the slip that will occur on each dislocation necessary to minimize stress energy in the medium. End effects are minimized by dividing each dislocation into 5 identical vertical sub-segments and calculating the mean slip on the ensemble. For short ruptures ($L \ll B$) the mean slip, d , is equal to the product of the elastic strain at failure, d/B , and the rupture length. This linear relation fails for dislocations that approach in length the breadth of the strain channel. For very long ruptures ($L \gg B$) slip approaches but cannot exceed the displacement of the plates, d . Figure 3 illustrates the resulting "knee" in the relation between slip and rupture length where these two processes overlap.

3D Strain-Channel:

The boundary conditions driving slip on shallow vertical faults in this model consist of a shear displacement on a vertical dislocation surface embedded in a half space below a locking depth (Figure 1b). We examine the displacements on rectangular frictionless fault segments with areas that increase as L^2 until they fill the vertical width of the plate boundary

Copyright 1994 by the American Geophysical Union.

Paper number 94GL02279

0094-8534/94/94GL-02279\$03.00

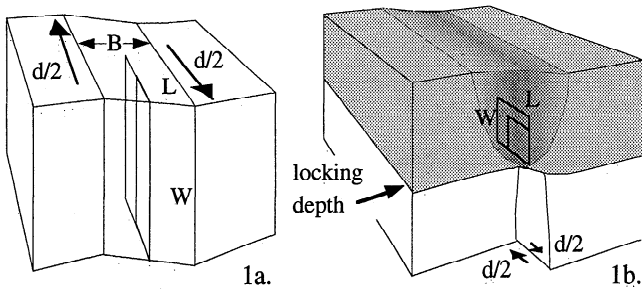


Fig. 1. a) 2D model: uniform strain is developed within an infinitely long elastic channel of breadth B by antisymmetric displacement, d , of two rigid plates of vertical thickness W . 1b) 3D model: displacement, d , is imposed on a vertical fault below some locking depth. Dashed lines indicate the narrowing of the resulting strain-channel with depth. For long ruptures, W is constant and equal to the locking depth.

seismogenic zone, equal to the locking depth, at which dimension W remains constant and further area-increase is proportional to L .

For short ruptures nucleating in the center of the seismogenic zone, displacement is linearly proportional to length. However, ruptures nucleating at the base of the seismogenic zone obey a more complex relation (Figure 3). As before, induced displacements increase slowly with length for ruptures much longer than the breadth of the strain-channel, and asymptotically approach the total displacement available at the plate boundary. The 3D model results for mid-crustal rupture are similar to the 2D results where the breadth of the 2D strain channel exceeds twice the locking depth of the 3D model (Figure 3).

Implications for Slip

The above 2D and 3D results provide a geometric explanation for the observed non-linear relation between the magnitude of a strike-slip earthquake and the displacements observed during rupture. The inflection in Figure 3 marks a change in mechanics between smaller earthquakes, for which co-seismic slip is much less than the instantaneous plate boundary displacement and which incompletely release strain within the plate boundary (resulting in a slip deficit), and great earthquakes, for which coseismic rupture may approach the instantaneous plate boundary displacement and which more completely release this strain. The transition magnitude for a change of length/magnitude scaling, is proportional to the locking depth of the inferred buried fault in the elastic plate. Thus for the thin brittle zone expected for a transform fault close to a rapid spreading ridge the transition will occur for lower magnitude earthquakes than for a transform remote from a slow ridge or for strike-slip faults in thick ancient elastic crust. However, the magnitude range is not large (<1) given

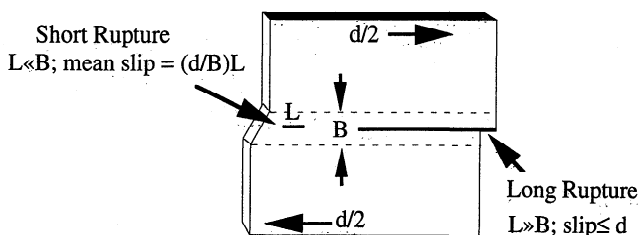


Fig. 2. Sketch illustrating displacements induced on dislocations in a 2D strain-channel (cf. Figures 1a and 3).

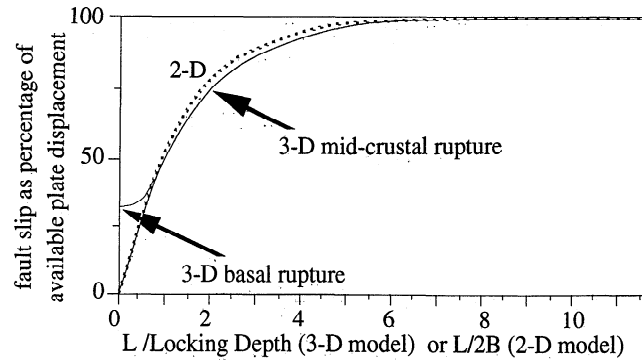


Fig. 3. Displacement as a function of rupture length for ruptures within 2D and 3D strain-channels. The "knee" in the curve occurs for ruptures with lengths similar to the breadth of the surface velocity field, B , which for California transform events corresponds to a fault length of ≈ 30 km.

that the width of vertical strike slip faults varies perhaps by less than a factor of 4 in these different environments. The strain at failure, which may vary by an order of magnitude, also modifies the slip and magnitude of the resulting earthquake.

The downward-tapering breadth of the strain field in the 3D model causes shear strain to increase within a narrowing volume toward the base of the plate. This implies that rupture is most likely to initiate near the base of the seismogenic layer, in accord with observations. Natural ruptures typically nucleate from the base of the crust and propagate toward the surface. The 3D model manifests a second feature that has its counterpart in nature. When rupture occurs at, say, a failure strain of 10^{-4} in the deepest 10% of our model fault, the shear strain applied to the shallowest 10% of the fault may be less than 10^{-3} , perhaps insufficient to sustain rupture near the surface. Previous studies of rupture nucleation have assumed uniform strain as a function of depth (Das and Scholz, 1983; Wallace and Wallace, 1993).

We examined the variable slip caused by the variation in the breadth of the strain-field with depth in the 3D strain channel model by dividing the frictionless vertical dislocation into several contiguous sub-segments. As before, each sub-segment is free to slip along-strike to minimize stress in the medium. We tested two models; in the first we examined the mean slip on dislocations of various areas located at the base of the elastic crust (*i.e.* with their lower edge at the locking depth), in the other we examined the slip on dislocations nucleating symmetrically from the center of the seismogenic zone. The mean slip at depth always exceeds slip near the surface (Figure 4), especially for ruptures nucleating from the base of the brittle crust. The two models are identical for ruptures that completely break the brittle crust.

A consequence of this result is that in general, for surface-rupturing events smaller than $M=7$, observed surface slip will be significantly less than that estimated from the geometric seismic moment. This finding implies that field data used to develop scaling laws (*e.g.* Scholz, 1982; Bonilla *et al.*, 1984) are systematically biased to smaller moments. For example, the mean slip on an $M=7$ event that fills the seismogenic zone is $\approx 50\%$ more than the largest observed surface displacement. Surface slip for shallow $M<7$ events are biased to low values or may be missing if, as mentioned above, surface shear strain is lower than needed to sustain rupture propagation.

A further consequence of the variation in slip with depth for small and moderate earthquakes is that a slip deficit will tend to develop near the surface. Although our models examine initial slip of an unruptured plate boundary, repeated slip in

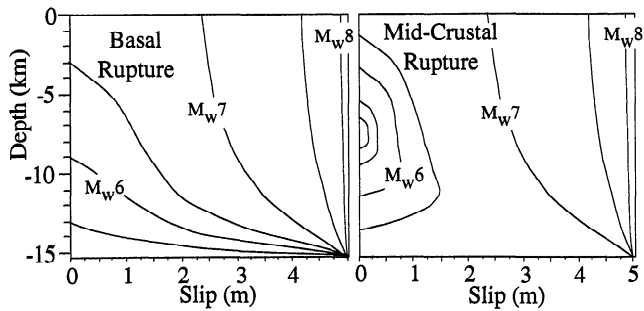


Fig. 4. Contours of mean slip at a given depth as a function of depth for vertical strike-slip ruptures propagating from the base of seismogenic zone (basal rupture) or from half the locking depth (mid-crustal rupture). Models driven, as in Figure 1b, by slip of 5m on a fault below a locking depth of 15 km. Small ruptures are squares with area L^2 , long ruptures are rectangular, with area LW (see Figure 1b). Approximate moment-magnitudes were determined from the definition of the scalar seismic moment, $M_0 = \mu * \text{slip} * L * W$ and the relation $M_w = 2/3 (\log M_0) - 10.7$ (using c.g.s. units).

moderate earthquakes within the plate boundary strain field will enhance the surface slip deficit. Because boundary conditions driving plate motion require that displacement should be uniform along-strike and throughout the vertical width of the plate boundary. This surface slip deficit must therefore be accommodated by additional seismic slip or near-surface elastic or inelastic deformation, presumably distributed over a wider area near the surface than near the base of the seismogenic zone. Alternatively, large earthquakes must occasionally occur to remove the surface slip deficit.

Discussion

Scaling relations

Rundle (1989) and Romanowicz and Rundle (1993) clarify the relation between so-called L- and W-scaling for rupture as follows: in L-scaling slip is linearly proportional to the length of the fault, and seismic moment increases with L^2 (Scholz, 1982), whereas in W-scaling, slip for all ruptures is proportional to the small dimension of a rupture (W) and seismic moment increases with LW . Our strain-driven model (an ϵ -model) accounts for changes in scaling without invoking processes that assume either L- or W-scaling. The observed magnitude/moment distribution among strike-slip earthquakes (Pacheco and Sykes, 1992) is a natural consequence of the inferred distribution of strain energy at the plate boundary. Our results suggest that a change in scaling will occur not for a unique rupture length, but will be manifest for a range of event magnitudes depending on the locking depth and strain at failure. Thus the resolution of the current debate concerning L- and W-scaling for transform plate-boundary slip requires careful normalization of the observational data. The debate is important because the relations form the basis for hazard analysis.

Independent tests of the ϵ -model are possible. The counter-intuitive, near-surface slip deficit accompanying moderate earthquakes is accessible through the analysis of coseismic geodetic data, or from observations of near-fault, vertical tilt. The angular rotation caused by slip at depth exceeding surface slip ($10\text{-}60 \mu\text{rad}$) can be observed by borehole tiltmeters, but not by long-baseline tiltmeters and spirit-leveling, which are sensitive only to horizontal tilts. Seismic radiation from moderate, strike-slip ruptures should also contain a significant torsional component in the plane of the fault.

Our 3D results are calculated assuming that slip occurs on square patches ($L < W$) or rectangular patches ($L > W$) of varying size. In practice the rupture zones of small and moderate earthquakes are irregular areas whose shapes are presumably moderated by frictional variations on the fault surface and by near-fault stress. The effect of friction is not considered in our study because frictional effects do not result in the accumulation of a slip deficit, except perhaps through their effect on inelastic deformation. We recognize, however, that changes in fault-zone rheology with depth may modify coseismic slip during rupture. We assume, moreover, that strain outside the strain-channel is unable to contribute to driving slip on the rupture. The effective contribution to coseismic slip of strain energy at great distances from a fault is limited by viscous coupling to underlying layers (Turcotte and Shubert, 1982), although this remote strain field may be important in driving aseismic slip.

Seismicity and the near-surface slip deficit

The decrease of shear strain driving a fault near the surface results in the accumulation of a surface slip deficit except near the center of very long ruptures (> 100 km). Near the ends of long ruptures, however, a surface slip deficit remains. This raises an important issue concerning patterns of seismicity following, or preceding, rupture in great transform earthquakes. We attribute the absence of seismicity near the central regions of the 1906 and 1857 ruptures during the interseismic period to the efficient annulment of slip deficit throughout the seismogenic zone by these events. According to our models, surface slip deficits remain near the ends of these great ruptures and it is expected that these will be most highly stressed near the end of the following interseismic period, resulting in increased moderate seismicity as the next great earthquake approaches (Sykes and Jaumé, 1990).

The shallow slip deficits our models predict are not manifest in the models of Rice (1993) of fault slip that incorporate depth-variable fault rheology because these examine the slip history of very long ruptures (240 km). Our results suggest that to model accurately the cumulative fault slip within a plate boundary, it is important to consider the effect of finite rupture lengths.

Aseismic fault creep

The creeping segment of the San Andreas fault in central California acts as a frictionless dislocation whose length is long compared to its width. Thus the cumulative distribution of aseismic creep resembles the distribution of slip during a great earthquake with similar dimensions. Our models predict no surface slip deficit near the center of the creeping zone, and the development of surface slip deficits near Parkfield and San Juan Bautista, consistent with our understanding of these regions.

Where moderate earthquakes are a characteristic feature of fault slip, such as on the Hayward fault, aseismic slip of the surface fault appears to provide a mechanism for complete compensation for the surface slip deficit predicted by our models (Savage and Lisowski, 1993). This is because the length of the creeping zone is large compared to the breadth of the surface strainfield. Although we have ignored the effects of viscous subcrustal rheologies, these effectively broaden the velocity field at depth, ultimately approximating the 2D driving conditions of Figure 1a that do not result in a surface slip deficit. Where recurrence rates are sufficiently rapid for the effects of viscous relaxation to be neglected, the simplest way for a transform fault zone to balance its deep and shallow slip budgets is for it occasionally to experience throughgoing rupture. This suggests that infrequent great earthquakes and/or

shallow aseismic fault slip may be necessary features of transform plate boundaries.

In this article we confine ourselves to examining the slip distribution on isolated ruptures within a transform boundary. Model experiments show that previous contiguous ruptures affect the surface deficit depending on their length. The presence of contiguous ruptures does not fundamentally alter our conclusions concerning short ruptures if the contiguous ruptures are also short. Only where contiguous failed segments are long will the slip on an intervening short segment be approximately uniform at all depths.

Conclusions

The velocity field observed geodetically at a plate boundary is interpreted as a downward-continuing strain field that may be rectangular or narrowing in breadth with depth. The amplitude of slip on fault ruptures within this strain field depends on the length of the rupture compared to the breadth of the strain field. The finite breadth of the strainfield causes a change in slope of the magnitude vs slip relation for earthquakes close to $M=7$. The change in scaling reflects both the effects of a change in area-growth from L^2 to LW , and a smooth variation in the relation between slip and rupture length. Both short and long ruptures are driven by strain, but the slip on long ruptures is limited by the available displacements.

The downward convergence of the strain field in the 3D model causes the elastic conditions driving slip during rupture to intensify with depth. As a consequence, ruptures nucleate at depth and slip reduces toward the surface, especially during moderate earthquakes ($M \leq 7$). This points to a systematic bias between observational and theoretical estimates of geometric seismic moment. In contrast, the central portions of great transform ruptures accommodate plate boundary slip throughout the seismogenic zone, consistent with the observation that these regions are effectively aseismic between great earthquakes. The terminal regions of these long ruptures, however, are associated with surface slip deficits that may be relieved throughout the earthquake cycle, and increasingly near the end of the interseismic period.

Small and moderate earthquakes result in a surface slip deficit. Aseismic surface slip can release this slip deficit if creep extends continuously along strike for distances large compared to the breadth of the zone of concentrated shear strain. Great earthquakes may be necessary features of plate boundaries to eliminate the surface slip deficit where creep is absent.

Acknowledgments. The research was funded by USGS 1434-93G-2356. We thank J. Gomberg and J. Rundle for discussions of early drafts, and 2 anonymous reviewers for helpful suggestions. J. Brune initiated our interest in seismic source scaling. CERI contribution 227.

References

- Bonilla, M.G., R.K. Mark, and J.J. Lienkamper, Statistical relations among earthquake magnitude, surface rupture length, and surface fault displacement, *Bull. Seism. Soc. Am.*, **74**, 2379-2411, 1984.
- Crouch, S.L. and A.M. Starfield, Boundary Element Methods in Solid Mechanics, *Allen & Unwin*, London, 320 pp., 1983.
- Das, S., and C.H. Scholz, Why large earthquakes do not nucleate at shallow depths, *Nature*, **305**, 621-623, 1983.
- Gomberg, J. and M. Ellis, Topography and tectonics of the central New Madrid seismic zone: results of numerical experiments using a three-dimensional boundary-element program, *J. Geophys. Res.*, in press, 1994.
- Lisowski, M., J.C. Savage, and W.H. Prescott, The velocity field along the San Andreas fault in central and southern California, *J. Geophys. Res.* **96**, 836389, 1991.
- Pacheco, J.F. and L. Sykes, Seismic moment catalog of large shallow earthquakes, *Bull. Seism. Soc. Am.*, **82**, 1306-1349, 1992.
- Pacheco, J.F., C. Scholz, and L. Sykes, Changes in frequency-size relationship from small to large earthquakes, *Nature*, **355**, 71-73, 1992.
- Rice, J.R., Spatio-temporal complexity of slip on a fault, *J. Geophys. Res.*, **98**, 9885-9907, 1993.
- Robaudo, S. and C.G.A. Harrison, Measurements of strain at plate boundaries using space-based geodetic techniques, *Geophys. Res. Lett.*, **20**, 1811, 1993.
- Romanowicz, B. and J. B. Rundle, On Scaling Relations for Large Earthquakes, *Bull. Seism. Soc. Amer.*, **83**, 1294-1297, 1993.
- Rundle, J., Derivation of the complete Gutenberg-Richter magnitude frequency relation using the principle of scale invariance, *J. Geophys. Res.*, **94**, 12337-12342, 1989.
- Scholz, C., Scaling laws for large earthquakes and consequences for physical models, *Bull. Seism. Soc. Am.*, **72**, 1-14, 1982.
- Savage, J.C., Equivalent strike-slip earthquake cycles in half-space and lithosphere-asthenosphere Earth models, *J. Geophys. Res.*, **95**, 4873-4879 1990.
- Savage, J.C., and M. Lisowski, Inferred depth of creep on the Hayward fault, Central California, *J. Geophys. Res.*, **98**, 787-793, 1993.
- Sykes, L.R. and S.C. Jaumé, Seismic activity on neighboring faults as a long-term precursor to large earthquakes in the San Francisco Bay area, *Nature*, **348**, 1990.
- Turcotte, D.L., and G. Schubert, *Geodynamics*, John Wiley and Sons, New York. 450 pp. 1982.
- Wallace, M.H., and T.C. Wallace, The paradox of the Loma Prieta earthquake: why did rupture terminate at depth? *J. Geophys. Res.*, **98**, 19859-19868, 1993.

P. Bodin, Center for Earthquake Research and Information, University of Memphis, Memphis TN 38152.

R. Bilham, CIRES and Department of Geological Sciences, University of Colorado, Boulder CO 80309

(Received: February 14, 1994; Revised June 29, 1994; Accepted August 9, 1994)